

Microrheological detection of protein unfolding

Raymond S. Tu and Victor Breedveld*

School of Chemical & Biomolecular Engineering, Georgia Institute of Technology, 311 Ferst Drive, N.W., Atlanta, Georgia 30332, USA

(Received 23 November 2004; revised manuscript received 2 June 2005; published 13 October 2005)

We apply passive probes to protein solutions and evaluate the viscous response to folding and unfolding, allowing us to accurately quantify both the thermodynamics of protein folding and the structural dimensions of the protein molecules with subnanometer resolution. Hard-sphere approximations predict a measurable change in relative viscosity as the hydrodynamic volume fraction of protein molecules increases during unfolding. Microrheology measures these changes to unambiguously evaluate the ensemble average characteristics of the unfolded state in a denaturant, urea, while minimizing the shear-induced unfolding and alignment associated with conventional rheometry.

DOI: [10.1103/PhysRevE.72.041914](https://doi.org/10.1103/PhysRevE.72.041914)

PACS number(s): 87.15.Cc, 83.85.Ei, 87.15.Vv

Probing the formation and stability of a tertiary structure from an entropically favored random coil is a fundamental challenge in defining our proteome and designing novel proteins [1]. The need for an accurate experimental characterization of proteins in their unique native state and denatured states has led to the development of a host of tools that facilitate the understanding of protein folding and stability.

Conventional techniques to evaluate protein (un)folding include binding (natural ligands or antibodies) and activity studies, spectroscopy (IR, fluorescence, circular dichroism, or NMR), proteolysis of exposed core amide bonds, scattering techniques (light, x-ray, or neutron), and separation techniques (chromatography or gel electrophoresis). Using these techniques has furthered our understanding of the dynamics associated with protein folding, but the “fully” unfolded state remains difficult to clearly define [2]. A denatured protein represents a large collection of states, and this ensemble of structurally fluctuating proteins is challenging to characterize using standard methods. Therefore, macroscopic properties, such as viscosity, can be employed to examine the average characteristics of the denatured state.

Rheological measurements have often been suggested as a strategy to evaluate folding phenomena, because the hydrodynamic volume of the protein molecules can be derived from hard sphere approximations to yield the relative compactness of the folded and unfolded states [3]. However, active shearing during experiments and the need for fairly large sample volumes has relegated viscometric characterization to a corroborative tool. Microrheology offers a methodology that obviates both these hurdles by monitoring the Brownian trajectories of colloidal probe particles embedded in microliter-sized samples. In this communication, we show that microrheological measurements of changes in protein solution viscosity upon the addition of denaturant allow one to quantitatively evaluate changes in size as the protein unfolds, as well as calculate the stability of that protein.

Relating the molecular dimensions of a protein to the intrinsic viscosity has been suggested numerous times in literature [4], but there are scant examples of the actual experi-

mental application of this method to biological macromolecules [5]. The underlying hypothesis is that globular proteins can be treated according to the hard-sphere theory first developed by Einstein [6] and later augmented by Batchelor [7]. The model predicts that the relative viscosity of a hard sphere suspension will vary as a quadratic function of volume fraction with the following coefficients:

$$\eta = \eta_s(1 + 2.5\phi + 6.2\phi^2), \quad (1)$$

where ϕ is the equivalent spherical volume fraction occupied by the protein, and η and η_s are the measured viscosity and the solute-free solvent viscosity, respectively. Batchelor's contribution accounts for two-body interactions, thus enabling an analysis at higher protein concentrations; however, this equation begins to underestimate the relative viscosity at volume fractions greater than 20% and when interparticle interactions are prominent [8].

Rheological changes associated with the collapse into compact three-dimensional structures in folding and aggregation (or quaternary structure) can potentially enumerate details of protein morphology, adding viscous and viscoelastic characterization to the proteomic toolbox. An impediment to measuring unfolding phenomena by monitoring changes in viscosity is that these measurements are typically made by applying external shear forces that can promote the premature loss of tertiary structure, thus artificially increasing the fraction of unfolded proteins and biasing the experiments. This effect requires significant shear stresses for fully folded proteins (~ 35 dyne/cm²), but will be exacerbated under conditions where the protein is already partially unfolded [9]. Passive microrheology uses thermal fluctuations and the resulting Brownian motion of probe particles to evaluate sample viscosity, circumventing the concern of shear-induced unfolding. The mean-squared displacement (MSD), $\langle \Delta \vec{r}(\tau)^2 \rangle$, of embedded spherical probes in a Newtonian fluid is described by the Stokes-Einstein equation:

$$\langle \Delta \vec{r}(\tau)^2 \rangle \equiv \langle |\vec{r}(t + \tau) - \vec{r}(t)|^2 \rangle = \frac{dk_b T}{3\pi\eta a} \tau, \quad (2)$$

where thermal energy, $k_b T$, promotes the displacement of spheres of radius a as a linear function of the lag time, τ . d is

*Electronic address: victor.breedveld@chbe.gatech.edu

the dimensionality of the trajectories (generally $d=2$ in microscopy) [10–12].

Microrheological measurements include several other qualities that make them well suited for the evaluation of biomolecules. Sample sizes are only constrained by the focal volume of a high magnification objective lens and hydrodynamic interactions of the probe particles with the sample boundaries, allowing assays of less than $1 \mu\text{L}$ [13]. Additionally, Freer *et al.* show the capacity for proteins to adsorb to interfaces, where exposure to a hydrophobic environment promotes unfolding and network formation, yielding elevated viscosities and elastic characteristics [14]. Our measurements localize the focal volume away from any free surfaces avoiding the elastic contributions observed at the interface. Microrheology also has the potential for high time resolution in kinetic measurements [10], using the ability of high-speed video analysis to detect minute changes in folded state as a function of changing solvent conditions. Finally, microrheology offers the facile coupling with high-throughput combinatorial methods through the use of standard multiwell plates, which are commonplace for the combinatorial synthesis of novel proteins and peptides. Individual measurements require the trajectories of >200 particles, which can be obtained in only 60 s. The bottleneck occurs with the image analysis, where the accurate determination of particle positions currently takes five minutes per measurement. Automation of the data analysis procedure should allow for approximately 250 measurements/day, which is sufficient to generate a “rheological phase diagram” for most biomacromolecules [15].

We tested the hard sphere microrheology hypothesis on a globular protein model system, bovine serum albumin (BSA). The addition of urea to BSA leads to well-documented and predictable unfolding behaviors, where spectroscopy (UV absorbance, circular dichroism, and fluorescence) and calorimetry have established that the chemical denaturation of BSA at neutral pH results in a random coil that neither aggregates nor adsorbs significantly (N.B.: this behavior is not consistent with thermal denaturation, where aggregation and adsorption are observed) [16,17]. All solutions of BSA (96%–99% purity, Sigma) are prepared in 0.15 M NaCl to approximate physiological electrolyte concentrations. Concentrated urea is added to BSA solutions to give a final urea concentration between 0.0 and 9.0 M, and $1.0 \mu\text{m}$ spherical latex probes (IDC) are added at dilute concentrations of $\sim 0.07\%$ (Mass %).

Samples are allowed to stand in urea solutions for at least 24 h before measurements to ensure an equilibrium unfolded state. BSA adsorption to amidine-functionalized latex particles is commonly observed [19,20], but we estimate for a monolayer that even at our lowest BSA concentrations $<1\%$ (mol %) of the albumin molecules can access the latex surface, which does not affect the overall concentration of the protein in solution, nor will an adsorbed monolayer significantly change the radius of the particles. To verify this, measurements were also run on PEG-functionalized (sterically stabilized) particles [18]. Both types of particles show the same results, indicating that protein adsorption does not influence solution viscosity.

Viscosities of protein solutions are determined as a func-

tion of urea concentration by evaluating the trajectories of amidine-functionalized fluorescent-latex particles and applying the Stokes-Einstein equation for the diffusion of the probe particles. Brownian motion is monitored with a Peltier-cooled video camera (Cohu Inc.) at 30 frames per second and recorded digitally using specialized acquisition software, OpenBox. Image analysis software (IDL, Research Systems Inc.) identifies the particle trajectories, tabulating the time evolution of particle positions [10]. Individual movies are 50 s long and include an average of 550 trajectories, where the average length of each trajectory is 2.22 s (or 133 individual steps). For all folded and unfolded protein solutions the linear scaling between MSD and τ is valid through all measurable times (data not shown). Subsequently, the slope ($\Delta\tau/\Delta\text{MSD}$) is used to calculate the viscosity η [see Eq. (2)]. Because of their proportional relationship, $\Delta\tau/\Delta\text{MSD}$ and η can be plotted for the same dataset using two different axes, as shown in Fig. 1.

Solvent viscosities are measured with both microrheology and conventional rheology, and both techniques give the same answer to within 2%. Also shown in Fig. 1 are the relative viscosities of protein solutions, where the sigmoidal curve (dashed line) represents the “all-or-none” behavior typically associated with cooperative denaturation. Each error bar is the standard deviation from five independent measurements.

For comparison, data from Uversky *et al.* is included in Fig. 1 (stars), where the redshift of intrinsic tryptophan fluorescence was used to quantify the unfolded fraction [21]. The unfolding results obtained via microrheology closely overlay the fluorescent technique. We believe that the sigmoidal unfolding curve measured by the redshift in intrinsic tryptophan fluorescence should correlate well with our rheological measurement, as the exposure of buried hydrophobic amino acids will likely correspond to an increasing hydrodynamic radius of the BSA. The unfolding midpoint $[\text{urea}]_{1/2} = 5.9 \text{ M}$ measured with microrheometry is comparable to the midpoint $[\text{urea}]_{1/2} = 6.4 \text{ M}$ from spectroscopy. In contrast, CD measurements would focus on the degradation of a secondary structure with an increasing denaturant, which can artificially suggest a more stable native state when secondary and tertiary structures are decoupled. Proteins such as the engrailed homeodomain fold in a hierarchical fashion, where extremely stable α helices can be maintained long after the tertiary structure has decayed [22].

Shifts in the populations of the native and denatured states are evaluated assuming a two-state model, described by the following equations:

$$K_{eq}(C) \equiv \frac{F_u(C)}{F_n(C)} = \frac{\eta_n(C) - \eta_x(C)}{\eta_x(C) - \eta_u(C)}, \quad (3)$$

$$\Delta G(C) = -RT \ln K_{eq}(C), \quad (4)$$

where the Gibbs free energy, $\Delta G(C)$, is derived from the equilibrium constant, K_{eq} . K_{eq} is the ratio of unfolded protein over native protein, F_u/F_n , determined from the viscosities in Eq. (2) of the η_n (native), η_u (unfolded), and η_x (intermediate-states). The application of Eqs. (3) and (4)

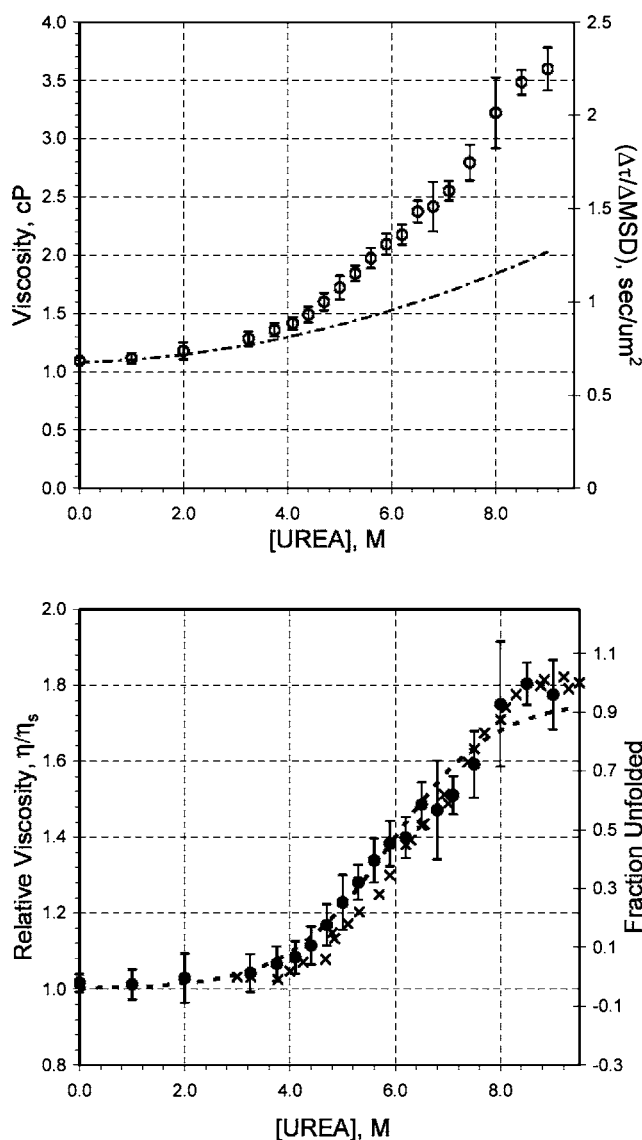


FIG. 1. Top, viscosity (\circ) of a 0.18 mM (1.8% volume fraction folded) BSA sample as a function of added urea, where the dashed line represents the solvent viscosity. Bottom, relative viscosity (\bullet) measurements show cooperative unfolding with increased urea, where the line represents a sigmoidal fit to the data. Data from Uversky *et al.* (\times) using an intrinsic Trp fluorescence technique is also included [21].

yields an equilibrium constant and a Gibbs free energy, respectively, where extrapolation to a zero concentration of urea gives the stability of the folded states, Fig. 2 [23]. Our analysis of BSA gives a Gibbs free energy of 15.5 ± 3.2 kJ/mol, which is within experimental error of literature values for Human Serum Albumin (HSA), 17.1 ± 4.2 kJ/mol, determined from fluorescence spectroscopy (HSA, 75.6% homology to BSA with conservative exchanges) [24]. The described characterization of free energy via changes in viscosity is general to any two-state unfolding process (and can be further extrapolated to unfolded intermediates with different hydrodynamic radii), but the application of a spherical model is required to obtain ensemble average dimensions of the unfolded state. Although BSA is a prolate

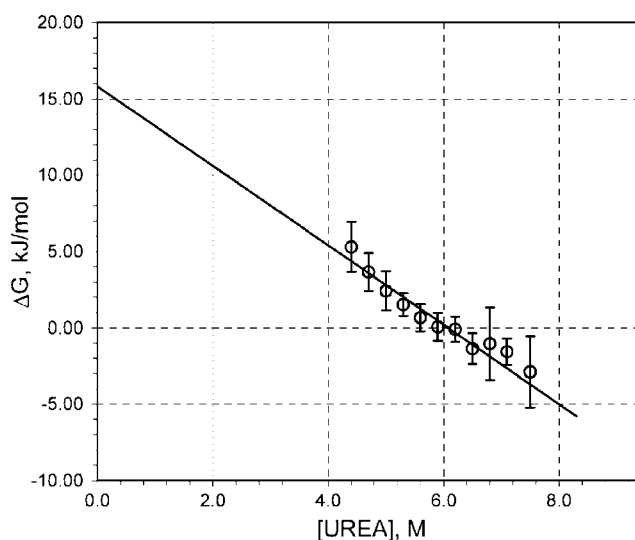


FIG. 2. Thermodynamic analysis of unfolding data. Extrapolation to the ordinate gives a free energy of unfolding, $\Delta G = 15.5 \pm 3.22$ kJ/mol.

ellipsoid with an axial ratio of 3.5:1 [25], our analysis approximates the viscous contribution of an equivalent suspension with a given effective Stokes radius, where the effective hydrodynamic radius is expected to be in between the lengths of the short and long axis of the prolate ellipsoid. This assumption is not suitable in conventional rheology, as flow fields will impart orientational ordering on axisymmetric shapes.

The hydrodynamic changes associated with unfolding modeled according to Eq. (1) assume a spherical geometry for the native state BSA and that denaturation does not engender significant aggregation or morphological changes. Using these assumptions, we evaluate the ensemble average effective hydrodynamic radius as a function of concentration (or volume fraction). Figure 3 shows the relative viscosity of solutions at various concentrations of BSA in a strongly denaturing solvent (7 M urea) and in a physiological equivalent solvent (0.15 M NaCl). The solid lines represent fits to Eq. (1), where the protein volume fraction is taken to be the product of concentration and the molecular volume. Coefficients are constrained to 2.5 and 6.2, leaving the molecular size as the only undefined variable. From this analysis, a hydrodynamic volume can be derived for any protein with a known molecular weight; for BSA this analysis yields radii of 75.3 ± 1.1 Å and 34.2 ± 1.4 Å for the unfolded and folded states, respectively. Equation (1) appears to fit the data over a wide range of concentration in 7 M urea, but unfolding data at higher concentrations should be interpreted cautiously, as 0.4 mM unfolded BSA represents a volume fraction of 40%. The data closely agree with the literature values from Uversky and Fink for denatured, 81.8, and native, 33.9 Å, BSA [21,26]. The methodology and error values for Uversky's measurements were not stated, and the authors of this paper are unaware of another study that quantifies the unfolded dimensions for BSA. Analogous viscosity measurements conducted on a conventional rheometer show exceptionally high viscosities (>100 cP) at low shear rates (<0.1 s $^{-1}$) and

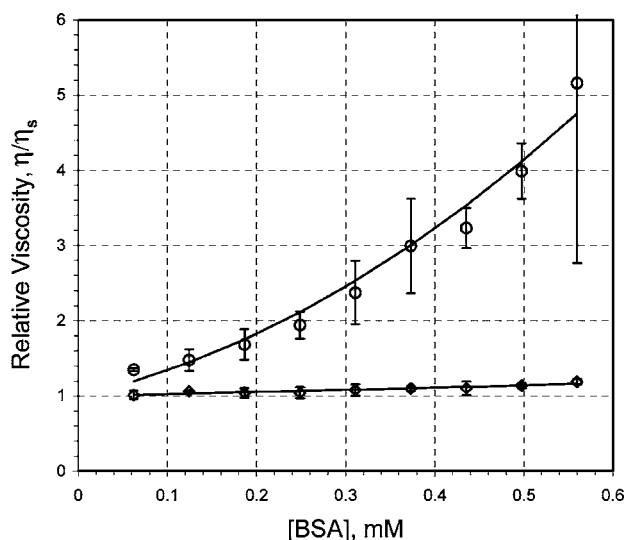


FIG. 3. Concentration-dependent viscosity measurements, fitted to Eq. (1) approximates the hydrodynamic radius of the folded (\diamond), 0 M urea, and unfolded (\circ), 7 M urea, states. $R_{folded}=34.2\pm 1.4 \text{ \AA}$ and $R_{unfolded}=75.3\pm 1.1 \text{ \AA}$.

shear-thinning behavior as the shear rate is increased (data not shown), which is probably due to the formation of an elastic protein layer at the air-water interface at the periphery of the cone-plate geometry [14]. The size determination with microrheology is capable of acquiring subnanoscopic length scales from macroscopic properties; moreover, it unequivocally characterizes the average dimensions of an ensemble of unfolded proteins. Additional experiments were done using a different protein, lysozyme, to establish the generality of this methodology. Data for both lysozyme and BSA agree with literature values for hydrodynamic radii, yet the authors should note that experiments with BSA show less particle aggregation than any other proteins tried. BSA is used as an idealized model to examine the folding and unfolding behavior in chemical denaturants, where the simple hard-sphere model can be applied to relate intrinsic viscosity to the molecular dimensions of individual molecules. Interacting protein systems or protein aggregation will certainly require more sophisticated models.

The correlation between viscosity and protein unfolding has been recognized for many years, but the application of conventional viscometry to study protein stability and denaturation has been eclipsed by other techniques, primarily spectroscopic and separation-based methods. Microrheology offers an exceptionally simplistic method to explore unfolding phenomena. The technique is capable of directly evaluating the loss of tertiary structure, avoiding many of the pit-

falls associated with the measurement of unfolding, and combining microrheology with hydrodynamic models allows us to obtain gross features of the molecule as it unfolds. A tertiary structure is defined as the unique three-dimensional arrangement of a linear amino-acid chain [27], and using this type of methodology approximates the changes in relative compactness as a protein transitions from its tertiary structure to a random coil, ignoring the details of molecular positions.

A chicken-egg paradigm can be used to describe the relationship between secondary and tertiary structure [26], where either secondary structure is a prerequisite for a tertiary structure (framework model) or the formation of a compact hydrophobic core promotes a native secondary structure (hydrophobic collapse). The current analysis by definition focuses directly on the decay of tertiary structure avoiding artifacts that arise from variations in the mechanism of folding and unfolding. This characterization of relative compactness is analogous to dimensional characterization methods such as dynamic light scattering or SANS with the Guinier approximation, but microrheological measurements call for considerably smaller sample volumes. Additionally, rheological methods do not require the use of D_2O for contrast matching as in SANS methods, which has been shown to have a significant effect on protein interactions [28].

Rheological measurements have always been a fundamental tool for the characterization of macromolecules, but they have remained sidelined as a corroborative technique in the field of protein folding. This work offers microrheology as a primary tool to evaluate unfolding events, using micro-sized probes to accurately detect molecular stability and subnanometer length scales. The evaluation of thermodynamic stability and unfolding midpoints is accomplished without a hydrodynamic model, but further details can be derived by assuming a simple geometry. Alternatively, details regarding the geometry and mechanical properties of aggregated folded states, such as actin fibers [29], or unfolded states, such as amyloid states, may be drawn from the rheological characteristics, despite the axiom that "morphology from rheology is theology." These results suggest that microrheology can be applied as a fundamental tool to directly access changes in the tertiary structure during unfolding, and efficacious coupling with high-throughput screening qualifies microrheology to contribute in defining the proteome or evaluating combinatorially designed proteins.

We thank Karsten Bartling and Ron Rousseau for providing the Bovine Serum Albumin. This work was supported by the GeorgiaTech Foundation.

- [1] M. A. Dwyer, L. L. Looger, and H. W. Hellinga, *Science* **304**, 1967 (2004).
 [2] T. E. Creighton, *Protein Function: A Practical Approach* (Oxford University Press, Oxford, 1997).
 [3] A. Fersht, *Structure and Mechanism in Protein Science* (W.H.

- Freeman and Company, New York, 1999).
 [4] C. Tanford, *Adv. Protein Chem.* **23**, 121 (1968).
 [5] P. L. Privalov, Y. V. Griko, S. Y. Venyaminov, and V. P. Kutysenko, *J. Mol. Biol.* **190**, 487 (1986).
 [6] A. Einstein, *Investigations on the Theory of Brownian Move-*

- ment* (Dover, New York, 1956).
- [7] G. K. Batchelor, *J. Fluid Mech.* **83**, 97 (1977).
- [8] J. C. van der Werff, C. G. deKruif, C. Blom, and J. Mellema, *Phys. Rev. A* **39**, 795 (1989).
- [9] C. A. Siedlecki *et al.*, *Blood* **88**, 2939 (1996).
- [10] J. C. Crocker and D. G. Grier, *J. Colloid Interface Sci.* **179**, 298 (1996).
- [11] T. G. Mason, K. Ganesan, J. H. van Zanten, D. Wirtz, and S. C. Kuo, *Phys. Rev. Lett.* **79**, 3282 (1997).
- [12] A. J. Levine and T. C. Lubensky, *Phys. Rev. Lett.* **85**, 1774 (2000).
- [13] J. C. Crocker, M. T. Valentine, E. R. Weeks, T. Gisler, P. D. Kaplan, A. G. Yodh, and D. A. Weitz, *Phys. Rev. Lett.* **85**, 888 (2000).
- [14] E. M. Freer, K. S. Yim, G. G. Fuller, and C. J. Radke, *J. Phys. Chem. B* **108**, 3835 (2004).
- [15] V. Breedveld and D. J. Pine, *J. Mater. Sci.* **38**, 4461 (2003).
- [16] T. Peters, *All About Albumin* (Academic, San Diego, 1996).
- [17] B. Farruggia and G. A. Pico, *Int. J. Biol. Macromol.* **26**, 317 (1999).
- [18] A. J. Kim, V. N. Manoharan, and J. C. Crocker, *J. Am. Chem. Soc.* **127**, 1592 (2005).
- [19] J. L. McGrath, J. H. Hartwig, and S. C. Kuo, *Biophys. J.* **79**, 3258 (2000).
- [20] M. T. Valentine *et al.*, *Biophys. J.* **86**, 4004 (2004).
- [21] V. N. Uversky *et al.*, *Biochemistry* **36**, 13638 (1997).
- [22] U. Mayor *et al.*, *Proc. Natl. Acad. Sci. U.S.A.* **97**, 13518 (2000).
- [23] G. I. Makhatadze, *J. Phys. Chem. B* **103**, 4781 (1999).
- [24] B. Farruggia and G. A. Pico, *Int. J. Biol. Macromol.* **26**, 317 (1999).
- [25] D. Bendedouch and S. H. Chen, *J. Phys. Chem.* **87**, 1473 (1983).
- [26] V. N. Uversky and A. L. Fink, *FEBS Lett.* **515**, 79 (2002).
- [27] H. Lodish *et al.*, *Molecular Cell Biology* (Scientific American Books, New York, 1995).
- [28] C. Gripon, L. Legrand, I. Rosenman, O. Vidal, M. C. Robert, and F. Boue, *J. Cryst. Growth* **178**, 575 (1997).
- [29] I. Y. Wong, M. L. Gardel, D. R. Reichman, E. R. Weeks, M. T. Valentine, A. R. Bausch, and D. A. Weitz, *Phys. Rev. Lett.* **92**, 178101 (2004).